

Probing axion-like particles with RF cavities separated by thin barrier

Dmitry Salnikov^{*} and Petr Satunin[†]

*Moscow State University, 119991 Moscow, Russia and
Institute for Nuclear Research, 117312 Moscow, Russia*

D. V. Kirpichnikov[‡]

Institute for Nuclear Research, 117312 Moscow, Russia

(Dated: May 9, 2024)

We address the Light-Shining-through thin Wall (LStinW) laboratory setup to estimate the axion-like particle (ALP) sensitivity of a two radio frequency (RF) cavities immersed in static magnetic field. We show that the sufficiently thin wall between cavities can lead the improved sensitivity of the purely laboratory probes of ALP in the mass range 10^{-6} eV $\lesssim m_a \lesssim 5 \times 10^{-5}$ eV.

I. INTRODUCTION.

Feebly-interacting particles (FIPs) [1] are hypothetical light particles which extremely weak interact with the Standard Model (SM) fields and may consist the dark matter component of the Universe or can be a mediator between Dark Matter and SM sector. The well motivated FIPs are photophilic: pseudoscalar axion-like-particle (ALP) [2, 3] and vector dark photon (DP) [4, 5]. Both of them can be tested with their interaction with Standard Model photons.

A typical strategy for probing FIPs (ALPs and DPs) implies both their production and detection in a laboratory, and usually called Light-Shining-through-Wall (LSW) experiments [6–11]. The LSW setups consist of two cavities separated by a non-transparent wall for ordinary photons. The FIPs are produced in the first cavity by a cavity electromagnetic mode (in case of DPs) or by an interaction of two electromagnetic field components (in case of ALPs).

Generated FIPs can pass through the wall and convert back to photons in the detection cavity. In the present paper, we focus on the purely laboratory LSW setup for probing ALPs that consists of two radio frequency (RF) cavities separated by thin barrier. We also show that regarding expected reach can be comparable with the the typical LSW laser-based experimental limits [12, 13]. Typically, LSW RF cavity experiments, such as CROWS [14], DarkSRF [15], imply that the FIPs emitter and receiver cavities are divided by a distance that is comparable to the typical size of the detector. This setup is mostly sensitive to FIPs mass less than the emitter mode frequency since the heavier FIPs are virtual and

their density exponentially decrease with the distance between cavities.

Recently the authors of [16] propose an idea that a sufficiently thin wall between cavities significantly improves the DP sensitivity of in the region of the sufficiently large DP mass, such that it can be considered as off-shell state (see also [17] for another cavity configuration). In this paper, we address the thin wall idea for probing ALPs in LSW experiments. In particular, we argue that employing the sufficiently low driven emitter frequency $\omega \lesssim 1$ GHz and thin barrier between cavities $d \ll 1/\omega$, one can achieve a large density of the ALP field. As a result this leads to the improved sensitivity in the off-shell ALP mas region $m_a \gtrsim \omega$, if one compares it with the LSW purely laboratory CROWS [14] experiment. We also show that the expected reach of suggested LStinW setup is complementary to the laser-based laboratory limits of ALPS-I [12] and OSQAR [13] experimental facilities.

This paper is organized as follows. In Sec. II we discuss the ALP electrodynamics. In Sec. III we derive main formulas in order to estimate the sensitivity of the LStinW setup to probe ALPs. In Sec. IV we discuss the numerical results for the expected sensitivity.

II. THE ALP ELECTRODYNAMICS

The Lagrangian describing coupling of ALPs and Standard model photons reads

$$\mathcal{L} \supset -\frac{1}{4} F_{\mu\nu} F^{\mu\nu} + \frac{1}{2} \partial_\mu a \partial^\mu a - \frac{1}{2} m_a^2 a^2 - \frac{1}{4} g_{a\gamma\gamma} a F_{\mu\nu} \tilde{F}^{\mu\nu}, \quad (1)$$

where $F_{\mu\nu}$ is the electromagnetic tensor and $\tilde{F}^{\mu\nu} = \frac{1}{2} \epsilon^{\mu\nu\alpha\beta} F_{\alpha\beta}$ is its dual, a denotes the ALP field, and $g_{a\gamma\gamma}$ is dimensional ALP-photon coupling.

The Lagrangian (1) implies that the equations for the

^{*} e-mail: salnikov.dv16@physics.msu.ru

[†] e-mail: petr.satunin@gmail.com

[‡] e-mail: dmbrick@gmail.com

ALP field and SM photon in vacuum read respectively,

$$(\partial_\mu \partial^\mu + m_a^2) a = g_{a\gamma\gamma} (\vec{E} \cdot \vec{B}), \quad (2)$$

$$(\vec{\nabla} \cdot \vec{E}) = \rho_a, \quad [\vec{\nabla} \times \vec{B}] = \vec{E} + \vec{j}_a, \quad (3)$$

where the density of charge ρ_a and current \vec{j}_a , induced by the ALP, read respectively as follows

$$\rho_a = -g_{a\gamma\gamma} (\vec{\nabla} a \cdot \vec{B}), \quad \vec{j}_a = g_{a\gamma\gamma} ([\vec{\nabla} a \times \vec{E}] + \dot{a} \vec{B}). \quad (4)$$

We note that Eq. (2) describes the ALP production by the typical combination of electromagnetic fields $\propto (\vec{E} \cdot \vec{B})$ in its right hand side. Contrary, both Eqs. (3) and (4) can be associated with the ALP conversion in the strong magnetic field that results in the generation of a resonantly enhanced signal EM mode in the detector.

III. LIGHT-SHINING-THROUGH THIN WALL SETUP

In this section we discuss the following benchmark experimental setup consisting of two RF cavities. We consider two equal cylindrical cavities of a radius R and length L , located coaxial end-by-end and separated by the thin barrier of a length $d \ll L$, see Fig. 1, left panel. Both cavities are immersed in the static magnetic field $B_{\text{ext}} = 3$ T along the cavities axis.

a. The ALP emission: the emitter cavity is pumped by TM_{010} electromagnetic mode $\vec{E}_{\text{em}}(\vec{x}) = \vec{e}_z E_0^{\text{em}} \mathcal{E}_z^{\text{em}}(\vec{x}) e^{-i\omega t}$, where $\omega = x_{01}/R$ is a driven frequency of the TM_{010} mode, x_{01} being a first zero of the Bessel function $J_0(x_{01}) = 0$, $E_0^{\text{em}} = 3$ MV/m = 0.01 T is a magnitude of the driven emitter electric field, $\mathcal{E}_z^{\text{em}}(\vec{x}) = \alpha J_0(\omega \rho)$ is a EM cavity eigen-mode that is normalized as

$$\int_{V_{\text{em}}} d^3 \vec{x} |\mathcal{E}_z^{\text{em}}(\vec{x})|^2 = V_{\text{em}},$$

that implies the normalization factor to be $\alpha = 1/|J_1(\omega R)|$.

The Eq. (2) for produced ALP field implies the following solution,

$$a(t, \vec{x}) = g_{a\gamma\gamma} E_0^{\text{em}} B_{\text{ext}} \int_{V_{\text{em}}} d^3 \vec{x}' \mathcal{E}_z^{\text{em}}(\vec{x}') \frac{e^{ik_a |\vec{x} - \vec{x}'| - i\omega t}}{4\pi |\vec{x} - \vec{x}'|}, \quad (5)$$

where $k_a = \sqrt{\omega^2 - m_a^2}$ are typical momenta of the produced ALPs; the integration is performed over the emitter volume V_{em} . One replaces ik_a with $-\kappa_a = -\sqrt{m_a^2 - \omega^2}$ in Eq. (5) for $m_a \gtrsim \omega$.

b. The ALP detection: Now we discuss the signal induced by the ALP field in the resonant *receiver* cavity which is a copy of the emitter cavity, so we would search

for exactly the same TM_{010} mode $\mathcal{E}_z^{\text{em}}(\vec{x}) = \mathcal{E}_z^{\text{rec}}(\vec{x})$ which is expected to be grown resonantly. In particular, the resonant amplitude of the receiver is characterized by the term [11, 19]

$$G = -\frac{Q_{\text{rec}}}{\omega_s} \cdot \frac{1}{V_{\text{rec}}} \int_{V_{\text{rec}}} d^3 x \mathcal{E}_{\text{rec}}^{z*}(\vec{x}) j_a^z(\vec{x}), \quad (6)$$

where Q_{rec} is a quality factor for the receiver eigenmode and V_{rec} is the volume of the receiver cavity, $\omega_s \simeq \omega$ is a frequency of the receiver signal eigenmode, and $\mathcal{E}_{\text{rec}}^z(\vec{x})$ is a dimensionless signal eigenmode, that reads $\mathcal{E}_{\text{rec}}^z(\vec{x}) = \alpha J_0(\omega \rho)$. The expression Eq. (6) reads

$$G = -ig_{a\gamma\gamma} \frac{Q_{\text{rec}} B_{\text{ext}}}{V_{\text{rec}}} \int_{V_{\text{rec}}} d^3 x \mathcal{E}_{\text{rec}}^{z*}(\vec{x}) a(\vec{x}), \quad (7)$$

where B_{ext} is a characteristic magnetic field of the detection cavity and $a(\vec{x})$ is a stationary part of Eq. (5). The typical signal power reads [17]

$$P_{\text{signal}} = \frac{\omega}{Q_{\text{rec}}} \frac{1}{2} |G|^2 V_{\text{rec}}. \quad (8)$$

Now let us estimate the sensitivity numerically as maximum output in the receiver cavity that is given by the Dicke radiometer equation, [20],

$$\text{SNR} = \frac{P_{\text{signal}}}{P_{\text{noise}}} \cdot \sqrt{t \Delta\nu}, \quad (9)$$

where t is an integration time for a signal, $\Delta\nu$ is its bandwidth and P_{noise} is a power of thermal noise which can be estimated as $P_{\text{noise}} \simeq T \Delta\nu$ in the limit $\omega \ll T$, where $T \simeq 1.5$ K is the typical temperature of the receiver. We consider the narrowest possible bandwidth of a pump generator, which can be as small as $\Delta\nu \simeq 1/t$ (see e. g. Refs. [11, 19] and references therein). The quality factor is chosen to be $Q_{\text{rec}} \simeq 10^5$ throughout the paper. Moreover, in the numerical estimate we conservatively set integration time to be $t \simeq 10^6$ s $\simeq 1$ year. We address the quantum description of the signal in Appendix A.

Let \vec{x}' and \vec{x} be the coordinates associated with the emitter and receiver frame respectively. In addition, let \vec{l} be the vector linking the origins of the frames of both emitter and receiver for the coaxial design of the experimental setup. In this case one has a simple link between them $\vec{x}' = \vec{l} + \vec{x}$. The vector linking the cavity frames would be then $\vec{l} = (0, 0, l_z)$. For that notation the distance between closest endcaps of the cavities is $d = l_z - L$.

In the following we rewrite G via the dimensionless form-factor \mathcal{G}

$$G = \mathcal{G} g_{a\gamma\gamma}^2 E_0^{\text{em}} B_{\text{ext}}^2 Q_{\text{rec}} V_{\text{em}} \omega,$$

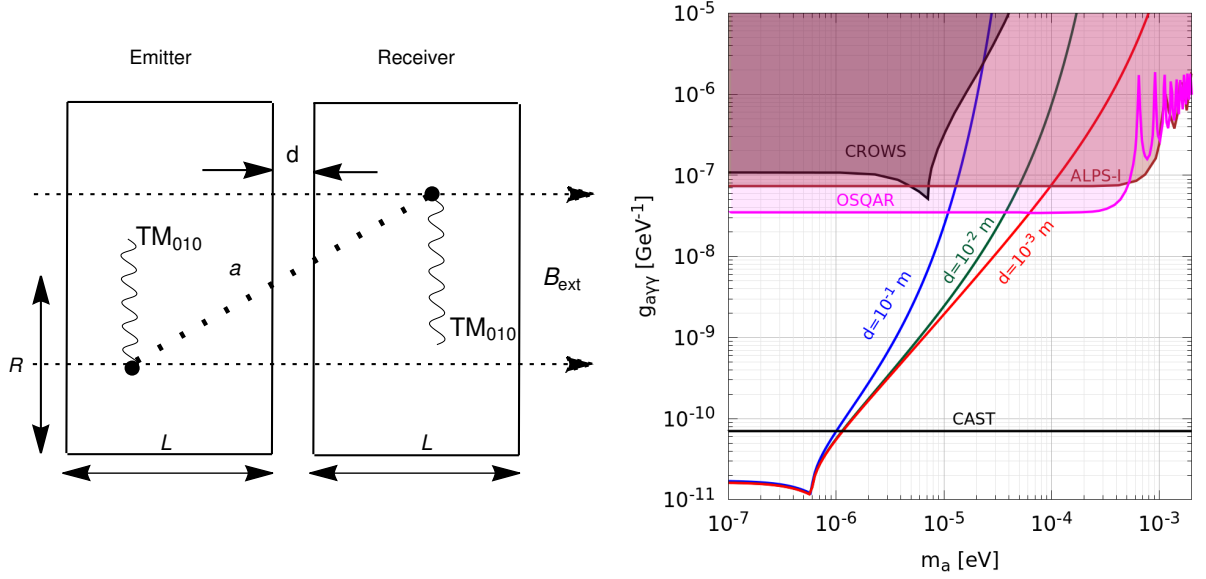


FIG. 1. *Left panel:* The typical scheme of LSthinW setup. *Right panel:* The setup sensitivity to ALP parameter space for TM_{010} mode. The blue, green, and red lines correspond to the barrier thickness of $d = 10$ cm, $d = 1$ cm, and $d = 1$ mm respectively, the radius and length of the cavities are chosen to be $R = 0.8$ m and $L = 1$ m, respectively. The purely laboratory bounds of CROWS [14], OSQAR [13], and ALPS-I [12] are shown by gray, magenta, and brown shaded region, respectively. The extraterrestrial helioscope limit of CAST [18] is shown by a solid black line.

where the expression for \mathcal{G} reads

$$\mathcal{G} = \int_{V_{\text{rec}}} \frac{d^3x}{V_{\text{rec}}} \int_{V_{\text{em}}} \frac{d^3x'}{V_{\text{em}}} \mathcal{E}_{\text{rec}}^{z*}(\vec{x}) \mathcal{E}_{\text{em}}^z(\vec{x}') \frac{e^{ik_a|\vec{x}-\vec{x}'-\vec{l}|}}{4\pi\omega|\vec{x}-\vec{x}'-\vec{l}|}. \quad (10)$$

Finally, by using Eqs. (8) and (9) we obtain the expected sensitivity,

$$g_{a\gamma\gamma} = \left[\frac{2T \text{SNR}}{\omega^3 Q_{\text{rec}} E_{0,\text{em}}^2 B_{\text{ext}}^4 V_{\text{em}}^2 V_{\text{rec}} |\mathcal{G}|^2} \right]^{\frac{1}{4}} \left(\frac{\Delta\nu}{t} \right)^{\frac{1}{8}}, \quad (11)$$

where the signal to noise ratio is chosen to be $\text{SNR} \simeq 5$ for the sensitivity estimate.

Remarkably, Eq. (10) can be rewritten in the following form [17]

$$\tilde{\mathcal{G}} = \frac{L^2 \alpha^2 [(\omega R) J_1(\omega R)]^2}{\omega V_{\text{rec}} V_{\text{em}}} \times \mathcal{I}, \quad (12)$$

where \mathcal{I} can be expressed through the 2D integral

$$\mathcal{I} = \int_0^\infty dk_\rho k_\rho \frac{J_0^2(k_\rho R)}{(k_\rho^2 - \omega^2)^2} \times \int_{-\infty}^\infty dk_z \frac{\sin^2(k_z L/2) e^{ik_z(d+L)}}{(k_z L/2)^2 (k_\rho^2 - [k_{A'}^2 - k_z^2 + i\varepsilon])}. \quad (13)$$

For the case of $k_a^2 \equiv \omega^2 - m_a^2 \gtrless 0$, the integration over k_z can be split into a sum of two terms, $\mathcal{I} = \mathcal{I}[k_\rho \gtrless k_a] + \mathcal{I}[k_\rho \lesssim k_a]$, where

$$\mathcal{I}[k_\rho \lesssim k_a] = \pi i k_a \int_0^1 dx \frac{J_0^2(k_a R \sqrt{1-x^2})}{(\omega^2 - k_a^2(1-x^2))^2} \times \frac{\sin^2(x k_a L/2)}{(k_a x L/2)^2} \exp(i x k_a l_z) \quad (14)$$

is a term for the typical integration region $k_\rho \lesssim k_a$ in Eq. (13) for the variable replacement $k_\rho = k_a(1-x^2)^{1/2}$, and

$$\mathcal{I}[k_\rho \gtrsim k_a] = \pi k_a \int_0^\infty dx \frac{J_0^2(k_a R \sqrt{1+x^2})}{(\omega^2 - k_a^2(1+x^2))^2} \times \frac{\sinh^2(x k_a L/2)}{(k_a x L/2)^2} \exp(-x k_a l_z) \quad (15)$$

is a term that is associated with the integration range $k_\rho \gtrsim k_a$ in Eq. (13), implying the variable redefinition $k_\rho = k_a(1+x^2)^{1/2}$ in the integrand. We note that both Eqs. (14) and (15) imply the variable redefinition $k_z =$

xk_a . Finally, for $\kappa_a^2 \equiv m_a^2 - \omega^2 \gtrsim 0$ one has

$$\mathcal{I} = \pi \kappa_a \int_1^\infty dx \frac{J_0^2(\kappa_a R \sqrt{x^2 - 1})}{(\omega^2 - \kappa_a^2(x^2 - 1))^2} \times \frac{\sinh^2(x \kappa_a L/2)}{(\kappa_a x L/2)^2} \exp(-x \kappa_a l_z), \quad (16)$$

where we use the integration variable replacement $k_\rho = \kappa_a(x^2 - 1)^{1/2}$.

IV. RESULTS AND DISCUSSION

In Fig. 1 (right panel) we show the setup sensitivity to ALP parameters $g_{a\gamma\gamma}$ and m_a . The expected reaches are shown for the barrier thickness in the range $1 \text{ mm} \lesssim d \lesssim 10 \text{ cm}$. For given benchmark design of the LStinW setup ($R \simeq 80 \text{ cm}$, $L \simeq 1 \text{ m}$) the resonant enhancement of the ALP sensitivity $g_{a\gamma\gamma} \lesssim 10^{-11} \text{ GeV}^{-1}$ can be achieved for the typical masses $m_a \simeq \omega \simeq 6 \times 10^{-6} \text{ eV}$. The expected reach for the sufficiently small ALP masses, $m_a \ll \omega$, can be at the level of $g_{a\gamma\gamma} \lesssim 2 \times 10^{-11} \text{ GeV}^{-1}$.

For the off-shell region of the ALP masses $m_a \gtrsim \omega$ one can achieve the enhancement of the sensitivity due to the reducing the cavity barrier thickness. In particular, Fig. 1 shows that the smaller the distance between the cavities d the smaller the slope of the expected reach curve. The setup with the benchmark thickness of the wall at the level of $d \simeq 1 \text{ mm}$ can rule out the typical masses of ALP below $m_a \lesssim 5 \times 10^{-5} \text{ eV}$. Moreover, the regarding region is complementary to the bounds of purely laboratory LWS setup, which are based on lasers.

In order to conclude this section we emphasize that one can employ the copper based cavities with typical skin depth of the order of $\delta \simeq 2 \mu\text{m}$ for $\omega \simeq 1 \text{ GHz}$. This conservatively implies that the typical barrier thickness can be as large as $d \gtrsim 30\delta \simeq 60 \mu\text{m}$, so that our benchmark value $d \simeq 1 \text{ mm}$ is a fairly reasonable wall thickness.

The possible extension of the present work can be addressed to a probing of millicharged and axion-like particles in LStinW setup by varying the cavity design, magnetic field orientation and the specific choice of the pump mode of the emitter, say TE_{011} . We leave these tasks for future study.

The code for numerical calculations and drawing figures can be shared upon request.

V. ACKNOWLEDGEMENTS

We would like to thank Maxim Fitkevich, Dima Levkov, Aleksandr Panin, Leysan Valeeva and Alexey Zhevlakov for fruitful discussions. This work is supported by RSF grant no. 21-72-10151.

Appendix A: Quantum description of the signal

Remarkably, that by employing Schwinger-Keldysh formalism [21, 22] one can link the coherent transition probability $P_{\gamma \rightarrow a \rightarrow \gamma}^{\text{coh}}$ with the averaged typical number of photon quanta in the receiver $\langle N_{\text{TM}_{010}} \rangle = \langle i | \hat{N}_{\text{TM}_{010}} | i \rangle = \langle i | \hat{a}_{\text{TM}_{010}}^\dagger \hat{a}_{\text{TM}_{010}} | i \rangle$, where the initial state $|i\rangle$ implies the time evolution from t_i to t_f and back to t_i

$$\langle N_{\text{TM}_{010}} \rangle = \int df' \int df'' \langle i | \hat{S}^\dagger | f' \rangle \langle f' | \hat{N}_{\text{TM}_{010}} | f'' \rangle \langle f'' | \hat{S} | i \rangle,$$

where \hat{S} is a S-matrix operator [22] for ALP-photon interaction, $|f'\rangle$ and $|f''\rangle$ represent the full set of states in theory at the moment t_f . Only $|f'\rangle = |f''\rangle$ states yield nonzero outcome, such that $\langle N_{\text{TM}_{010}} \rangle = P_{\gamma \rightarrow a \rightarrow \gamma}^{\text{coh}}$, implying a small number of mode quanta in a steady regime $\langle N_{\text{TM}_{010}} \rangle \lesssim 1$. In addition, we note that the straightforward analytical calculation reveals a well known result [19] for which the classical number of signal photons in the emitter $N_{\text{TM}_{010}} = Q_{\text{rec}} P_{\text{sign}} / \omega^2$ is $N_{\text{TM}_{010}} = \langle N_{\text{TM}_{010}} \rangle$.

-
- [1] C. Antel *et al.*, “Feebly-interacting particles: FIPs 2022 Workshop Report,” *Eur. Phys. J. C* **83**, 1122 (2023), [arXiv:2305.01715 \[hep-ph\]](#).
 - [2] Peter Svrcek and Edward Witten, “Axions In String Theory,” *JHEP* **06**, 051 (2006), [arXiv:hep-th/0605206](#).
 - [3] Asimina Arvanitaki, Savas Dimopoulos, Sergei Dubovsky, Nemanja Kaloper, and John March-Russell, “String Axiverse,” *Phys. Rev. D* **81**, 123530 (2010), [arXiv:0905.4720 \[hep-th\]](#).
 - [4] L. B. Okun, “LIMITS OF ELECTRODYNAMICS: PARAPHOTONS?” *Sov. Phys. JETP* **56**, 502 (1982).
 - [5] Bob Holdom, “Two U(1)’s and Epsilon Charge Shifts,” *Phys. Lett. B* **166**, 196–198 (1986).
 - [6] P. Sikivie, “Experimental Tests of the Invisible Axion,” *Phys. Rev. Lett.* **51**, 1415–1417 (1983), [Erratum: *Phys.Rev.Lett.* 52, 695 (1984)].
 - [7] A. A. Anselm, “Arion \leftrightarrow Photon Oscillations in a Steady Magnetic Field. (In Russian),” *Yad. Fiz.* **42**, 1480–1483 (1985).
 - [8] K. Van Bibber, N. R. Dagdeviren, S. E. Koonin, A. Kerman, and H. N. Nelson, “Proposed experiment to produce and detect light pseudoscalars,” *Phys. Rev. Lett.* **59**, 759–762 (1987).

- [9] F. Hoogeveen, “Terrestrial axion production and detection using RF cavities,” *Phys. Lett. B* **288**, 195–200 (1992).
- [10] Dmitry Salnikov, Petr Satunin, D. V. Kirpichnikov, and Maxim Fitkevich, “Examining axion-like particles with superconducting radio-frequency cavity,” *JHEP* **03**, 143 (2021), [arXiv:2011.12871 \[hep-ph\]](#).
- [11] Christina Gao and Roni Harnik, “Axion searches with two superconducting radio-frequency cavities,” *JHEP* **07**, 053 (2021), [arXiv:2011.01350 \[hep-ph\]](#).
- [12] Klaus Ehret *et al.*, “New ALPS Results on Hidden-Sector Lightweights,” *Phys. Lett. B* **689**, 149–155 (2010), [arXiv:1004.1313 \[hep-ex\]](#).
- [13] R. Ballou *et al.* (OSQAR), “New exclusion limits on scalar and pseudoscalar axionlike particles from light shining through a wall,” *Phys. Rev. D* **92**, 092002 (2015), [arXiv:1506.08082 \[hep-ex\]](#).
- [14] M. Betz, F. Caspers, M. Gasior, M. Thumm, and S. W. Rieger, “First results of the CERN Resonant Weakly Interacting sub-eV Particle Search (CROWS),” *Phys. Rev. D* **88**, 075014 (2013), [arXiv:1310.8098 \[physics.ins-det\]](#).
- [15] A. Romanenko *et al.*, “New Exclusion Limit for Dark Photons from an SRF Cavity-Based Search (Dark SRF),” (2023), [arXiv:2301.11512 \[hep-ex\]](#).
- [16] Asher Berlin, Roni Harnik, and Ryan Janish, “Light Shining Through a Thin Wall: Evanescent Hidden Photon Detection,” (2023), [arXiv:2303.00014 \[hep-ph\]](#).
- [17] Dmitry Salnikov, Petr Satunin, Leysan Valeeva, and D. V. Kirpichnikov, “Light-shinning-through-thin-wall radio frequency cavities for probing dark photon,” (2024), [arXiv:2402.09899 \[hep-ph\]](#).
- [18] V. Anastassopoulos *et al.* (CAST), “New CAST Limit on the Axion-Photon Interaction,” *Nature Phys.* **13**, 584–590 (2017), [arXiv:1705.02290 \[hep-ex\]](#).
- [19] Zachary Bogorad, Anson Hook, Yonatan Kahn, and Yotam Soreq, “Probing Axionlike Particles and the Axiverse with Superconducting Radio-Frequency Cavities,” *Phys. Rev. Lett.* **123**, 021801 (2019), [arXiv:1902.01418 \[hep-ph\]](#).
- [20] R. H. Dicke, “The Measurement of Thermal Radiation at Microwave Frequencies,” *Rev. Sci. Instrum.* **17**, 268–275 (1946).
- [21] Dmitrii A. Trunin, “Enhancement of particle creation in nonlinear resonant cavities,” *Phys. Rev. D* **107**, 065004 (2023), [arXiv:2209.10462 \[hep-th\]](#).
- [22] Ilia Kopchinskii and Petr Satunin, “Resonant generation of electromagnetic modes in nonlinear electrodynamics: Quantum perturbative approach,” (2023), [arXiv:2304.10209 \[quant-ph\]](#).